Available online at www.sciencedirect.com
ScienceDirect
Carbohydrate Research 343 (2008) 626–635
Carbohydrate RESEARCH

Promotion by phosphate of Fe(III)- and Cu(II)-catalyzed autoxidation of fructose

Glen D. Lawrence,[a,*] Ahmet Mavi[b] and Kadem Meral[c]

[a]*Department of Chemistry and Biochemistry, Long Island University, Brooklyn, NY 11201, USA*
[b]*Kazim Karabakir Education Faculty, Chemistry Education, Ataturk University, 25240 Erzurum, Turkey*
[c]*Department of Chemistry, Arts and Sciences Faculty, Ataturk University, 25240 Erzurum, Turkey*

Received 26 September 2007; accepted 18 December 2007
Available online 25 December 2007

Abstract—Although the oxidative destruction of glucose and fructose has been studied by several investigators over the past century, the mechanism by which phosphate promotes these oxidation reactions is not known. A wide range of oxidation products have been used to monitor the oxidation of sugars and free radicals have been shown to be involved. The influence of phosphate concentration on the rate of production of free radicals and several sugar oxidation products has been studied. It was found that fructose is much more susceptible to autoxidation than glucose, galactose, or sucrose. The promotion of sugar oxidation by phosphate was found to be iron dependent. Addition of the iron chelators, diethylenetriaminepentaacetic acid (DTPA) and desferrioxamine completely suppressed the oxidation reactions, even at high concentrations of phosphate. Formaldehyde was positively identified as a product of fructose oxidation by HPLC analysis of its acetylacetone adduct. A mechanism is proposed in which phosphate cleaves the oxo bridges of the iron(III)–fructose complex, based on UV spectral analysis and magnetic susceptibility measurements, and thereby catalyzes the autoxidation of fructose.

Keywords: Iron(III)–fructose complex; Magnetic susceptibility; Fructose oxidation; Formaldehyde; α-Dicarbonyls; Phosphate; Catalysis

1. Introduction

There has been growing concern that dietary fructose, particularly high fructose corn syrup in beverages, may be a factor in the epidemic of obesity and its associated health complications in the US population.[1,2] Animal models have demonstrated that high fructose consumption induces insulin resistance, hypertriglyceridemia, and hypertension, which are among the metabolic abnormalities associated with syndrome X or metabolic syndrome in humans.[2] Many studies have also shown an association between high fructose consumption and risk for coronary heart disease.[3] Many of these metabolic effects may be related to the pro-oxidant effects of fructose, since vitamin E was shown to have a protective effect on insulin sensitivity and the antioxidant status of high fructose fed rats.[4] It has been shown that fructose promotes the formation of advanced glycation end products (AGEs) more than glucose, and enhances free radical generation and associated degeneration of proteins and lipids more than glucose.[5]

It has been known since the early 20th century that fructose is much more susceptible to autoxidation than glucose and that phosphates promote their oxidation.[6,7] It was later found that traces of impurities in phosphate salts were responsible for this catalytic effect by phosphate.[8] It was likely that iron was the factor removed by multiple recrystallization of the phosphate salts, since Spoehr[6] had shown that iron-pyrophosphate was highly effective in catalyzing carbohydrate autoxidation. The relative order of reactivity toward oxidation would seem

Abbreviations: DTPA, diethylenetriaminepentaacetic acid; EDTA, ethylenediaminetetraacetic acid; NBT, nitrobluetetrazolium; NMR, nuclear magnetic resonance; SOD, superoxide dismutase; TBA, thiobarbituric acid; TBARS, thiobarbituric acid reactive species

* Corresponding author. Tel.: +1 718 4881452; fax: +1 718 4881465; e-mail: lawrence@liu.edu

0008-6215/$ - see front matter © 2007 Elsevier Ltd. All rights reserved.
doi:10.1016/j.carres.2007.12.016

surprising from the simple consideration that glucose is an aldose, whereas fructose is a ketose. However, hemiacetal formation produces a very stable pyranose ring structure in the case of glucose, which retards its reactivity as an aldehyde. Indeed, D-glucose is one of the least reactive sugars in nature in terms of Schiff base formation with amino groups in proteins.[9] On the other hand, fructose exists in both pyranose and furanose hemiketal forms, as well as the open chain keto form in solution. It is not clear what makes fructose more reactive toward autoxidation compared to glucose.

One of the first characterizations of an iron–fructose complex was reported by Charley et al.[10] The magnetic behavior of the Fe(III)–fructose complex indicated the formation of an antiferromagnetically coupled dimeric species at neutral pH, with hydrolysis of the oxygen bridges under more alkaline conditions.[11] The glucose complex with Fe(III) appears to be mononuclear.[12] ^{13}C NMR spectroscopy was used to show that Fe(III) binds preferentially to the β-pyranose form of fructose, which is the dominant form in aqueous solution,[13] whereas Cu(II) binds preferentially to a furanose form of fructose.[14] We report here several factors involved in accelerating the reactivity of fructose toward autoxidation and its promotion of oxidation reactions to better understand the mechanisms involved in the relatively high reactivity of fructose. It is shown that formaldehyde is a major product of fructose degradation, in addition to other reactive intermediates. The nature of the catalytic effect by phosphate in the presence of iron has been explored by spectroscopic techniques and a proposed mechanism is discussed.

2. Results

2.1. Lipid peroxidation

It was found that 10 mM fructose in the presence of liposomes prepared from soy lecithin would promote lipid peroxidation, as measured by thiobarbituric acid reactive species (TBARS) giving absorbance at 535 nm. Fructose oxidation products (in the absence of lipid) were found to produce a yellow colored product in the reaction with TBA. These yellow products had an absorbance maximum at about 430 nm and absorbance at 535 nm was less than 10% of the observed absorbance when liposomes were present (data not shown).

There was a steady increase in peroxidation of liposome mixtures over a period of two days in the absence of added metals or when iron or copper was added (Fig. 1). However, the Cu(II) catalyzed reactions showed a rapid increase in the first two days, followed by a gradual decrease in TBARS at 4 and 6 days. The iron catalyzed reaction showed a slower rate of peroxidation in the first two days, but continued to increase through day 6. In the absence of added metal ions, the production of TBARS in liposome mixtures containing 10 mM glucose was increased by a factor of 1.2 over a period of 2 days compared to control liposome mixtures containing no sugar or added metals (Fig. 1). By comparison, 10 mM fructose produced a 2.9-fold increase in TBARS relative to the control mixture in this time period.

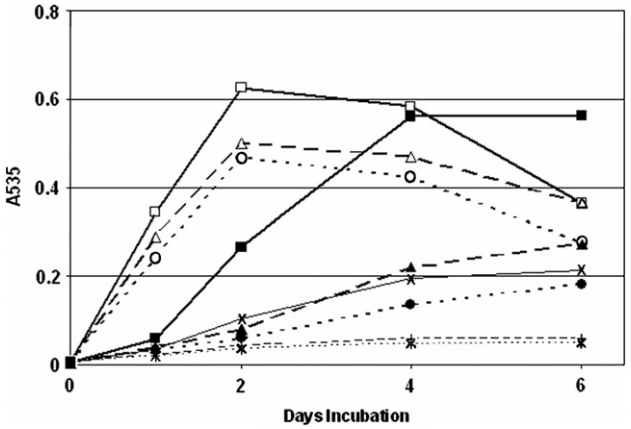

Figure 1. Lipid peroxidation without added metal ions (∗, +, X), or catalyzed by 20 μM $FeCl_3$ (solid markers) or 20 μM $CuSO_4$ (open markers) and with no added sugar (···∗···, ···●···, ···○···), with 10 mM glucose (--+--, --▲--, --△--), or with 10 mM fructose (—X—, —■—, —□—). The absorbance at 535 nm (A535) corresponds to thiobarbituric acid reactive substances in the liposome mixtures.

When 20 μM $FeCl_3$ or 20 μM $CuSO_4$ was added to the liposomes, there was a 1.7-fold and 13-fold increase in TBARS, respectively, compared to control liposomes (no metal added) over an incubation period of 6 days at 40 °C (dotted lines shown in Fig. 1). Addition of 10 mM fructose in the presence of added metals resulted in a further increase in TBARS of 4.5-fold and 1.3-fold in two days for Fe(III) and Cu(II), respectively. Addition of 10 mM glucose resulted in a much smaller increase in production of TBARS compared to 10 mM fructose in all cases (see Fig. 1).

2.2. Free radical production

It was suspected that free radical production in the process of oxidative degradation of these sugars was promoting lipid peroxidation. Sodium benzoate was used as hydroxyl radical scavenger, which yields salicylate and its *meta*- and *para*-isomer as fluorescent products. When fructose was added to solutions containing 5 mM sodium benzoate there was a dramatic increase in relative fluorescence ($\lambda_{ex} = 298$ nm, $\lambda_{em} = 403$ nm) indicating hydroxyl radical (or its equivalent in oxidizing properties) production. The amount of fluorescence was found to be dependent on several factors, including pH, concentration of phosphate, oxygen, and redox-active metals, such as iron, copper, and vanadium.

Metal chelating agents that suppress the redox activity, particularly of iron, inhibited hydroxyl radical production (see Table 1). Interestingly, both DTPA and desferrioxamine almost completely suppressed OH production, whereas EDTA exhibited only a moderate ability to suppress OH production. In the case where 100 μM EDTA was added along with 50 μM $FeCl_3$, there was actually a large increase in formation of fluorescent products relative to the sample where no iron nor metal chelator was added.

Addition of amino acids glycine and arginine had no significant effect on OH production, whereas addition of lysine augmented OH production by a small but significant ($p < 0.02$) amount (Table 2). Addition of 10 mM citrate inhibited OH production by 17%, whereas addition of 20 mM acetate increased OH production by 41% (Table 2). The amount of fluorescent products generated by glucose (7.97), galactose (11.3), and sucrose (1.18) was much less than that generated by fructose (59.0) under the same conditions in 50 mM phosphate buffer, pH 6, with 50 μM $FeCl_3$ being added. When solutions were sealed in a tube with a rubber septum and made anaerobic by purging with purified N_2 prior to incubation, the production of OH radical was diminished (Table 2).

Because the production of fluorescent products from benzoate was dependent on oxygen in the reaction mixture, it seemed likely that superoxide radical would be an intermediate. When nitroblue tetrazolium (NBT), a superoxide radical scavenger, was added to 20 mM

Table 1. Effects of metals and chelating agents on hydroxyl radical production by fructose and glucose in phosphate buffers[a]

Condition	Relative fluorescence[b]	
	Fructose	Glucose
10 mM phosphate (PBS)	11.8 ± 2.0	0.54 ± 0.15
20 mM phosphate	20.2 ± 12.0	1.50 ± 0.34
50 mM phosphate	34.7 ± 5.7	5.17 ± 1.20
100 mM phosphate	74.3± 16.5	12.8 ± 1.8
PBS + 20 μM $FeCl_3$	9.9 ± 3.7	0.47 ± 0.27
PBS + 10 μM $CuSO_4$	35.0 ± 1.5	7.19 ± 0.56
PBS + 0.10 mM EDTA	3.12 ± 0.68	
PBS + 0.10 mM DTPA	0.49 ± 0.28	
PBS + 0.10 mM EDTA + 0.05 mM $FeCl_3$	29.6 ± 2.8	
PBS + 0.10 mM DTPA + 0.05 mM $FeCl_3$	0.83 ± 0.11	
PBS with no sodium benzoate added	0.12 ± 0.09	0.09 ± 0.02
PBS with sodium benzoate but no sugar added	0.24 ± 0.02	

[a] Reaction mixtures contained 5.0 mM sodium benzoate and 10 mM fructose or 10 mM glucose with other additions of $FeCl_3$, $CuSO_4$, EDTA, or DTPA, as indicated and phosphate buffer, pH 7.4, at the designated concentrations. Reaction mixtures were incubated in triplicate for 9 days at 40 °C. Values are average ± standard deviation.

[b] Relative fluorescence of hydroxylated benzoate products was measured with excitation at 298 nm and emission at 403 nm.

Table 2. Effect of air, amino acids, citrate, acetate, and varying Fe(III) ion concentration on hydroxyl radical generation and α-dicarbonyl production[a]

Condition	Relative fluorescence[b]	α-Dicarbonyl production[c] (A_{295})
20 mM fructose		
0 μM $FeCl_3$ added	33.9 ± 4.0	0.223 ± 0.022
50 μM $FeCl_3$ added	59.0 ± 5.8	0.442± 0.016
150 μM $FeCl_3$ added	38.9 ± 3.1	0.384 ± 0.018
500 μM $FeCl_3$ added	7.52 ± 1.33	0.303 ± 0.008
1500 μM $FeCl_3$ added	0.80 ± 0.19	0.419 ± 0.335
Anaerobic + 50 μM $FeCl_3$	6.34 ± 0.81	0.164 ± 0.022
+5 mM glycine + 50 μM $FeCl_3$	63.8 ± 4.7	0.489 ± 0.016
+5 mM arginine + 50 μM $FeCl_3$	60.1 ± 0.8	0.281 ± 0.003
+5 mM lysine + 50 μM $FeCl_3$	72.3 ± 0.8	0.656 ± 0.019
+20 mM acetate + 50 μM $FeCl_3$	83.2 ± 1.0	0.775 ± 0.057
+10 mM citrate + 50 μM $FeCl_3$	48.3 ± 3.2	0.158 ± 0.003
Other sugars replacing fructose		
20 mM glucose + 50 μM $FeCl_3$	7.97 ± 7.2	0.086 ± 0.006
20 mM galactose + 50 μM $FeCl_3$	11.3 ± 7.9	0.115 ± 0.007
20 mM sucrose + 50 μM $FeCl_3$	1.18 ± 0.87	0.017 ± 0.001

[a] Reaction mixtures contained 20 mM fructose, or other sugars, 5.0 mM sodium benzoate in 50 mM phosphate buffer, pH 6.0, with other additions as indicated. Reaction mixtures were incubated in triplicate for 4 days at 40 °C. Values are averages ± standard deviation.

[b] Relative fluorescence of hydroxylated benzoate products was measured with excitation at 298 nm and emission at 403 nm.

[c] α-Dicarbonyl products were measured by reaction with Girard-T reagent and absorbance measured at 295 nm.

fructose solutions, the solutions turned blue in 24 h, indicating that O_2^- was produced. When 20 mM glucose or galactose was added under the same conditions in 50 mM phosphate buffer at pH 7.0, the NBT solutions remained yellow. It was found that dilution of formazan containing solutions in dimethyl sulfoxide would dissolve the blue precipitate for better quantitative measurements. Addition of superoxide dismutase (SOD) to solutions containing 20 mM fructose in 50 mM phosphate buffer at pH 7.0 inhibited the production of blue formazan in these reaction mixtures by 80%, relative to solutions without added SOD, indicating that O_2^- was responsible for the reduction of NBT (Fig. 2).

2.3. Analysis of fructose oxidation products

Many different products have been measured in the oxidative degradation of sugars, particularly of fructose and glucose. It was of interest to see what conditions in the reaction mixtures of fructose would favor one product or another. The production of α-dicarbonyls, formaldehyde, lactones, and acids was compared for variations in pH. It was found that there is some correlation for the amounts of these various products over the pH range studied, although the amount of lactone production falls off as pH increases above neutrality due to the shift in equilibrium for lactone formation, favoring the free acid under more alkaline conditions. Consequently, there was a sharp rise in acid production between pH 6 and pH 7, due to the increased rate of fructose oxidation combined with a shift away from lactone formation under alkaline conditions (Fig. 3).

The pH dependence for fructose oxidation was similar whether Fe(III) or Cu(II) was added (Fig. 4). The level of formaldehyde and glyoxal production was similar for the iron and copper catalyzed reactions, whereas lactone production and acid production were about 30% higher for the copper catalyzed compared to the iron catalyzed reactions. The decrease in formaldehyde levels between pH 6 and pH 7 in the presence of Cu(II) is probably due to the greater reactivity of copper toward aldehydes under alkaline conditions. Formaldehyde production at pH 6 was nearly the same for the iron and copper catalyzed reactions. Vanadium (10 μM V_2O_5) was added to some reaction mixtures with fructose and found to give similar levels of oxidation products as 20 μM Fe(III) or Cu(II) at pH 6 (data not shown).

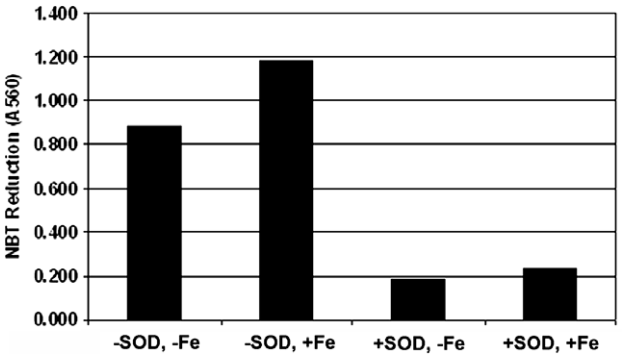

Figure 2. Inhibition of NBT reduction by superoxide dismutase. Solutions contain 50 mM phosphate, 10 mM tris buffer, pH 8.0, with (+) or without (−) SOD. Each reaction mixture contains 0.50 mM NBT and 20 mM fructose, with (+) or without (−) 50 μM $FeCl_3$. The amount of SOD added gave >90% inhibition of 6-hydroxydopa autoxidation in separate assays.

Formaldehyde was identified in the reaction mixtures by using HPLC separation of the products of the Hantzsch reaction with Nash reagent. The formaldehyde adduct with acetylacetone and ammonium ion gave a peak at 14.7 min, which was proportional to formaldehyde concentration used in the formation of the adduct (from 0 to 0.8 mM HCHO in standard solutions). The adduct formed in the fructose oxidation mixtures also gave a major peak at 14.7 min and the level of this peak correlated with the absorbance measurements at 412 nm in the spectrophotometric assay in the few samples that were analyzed by HPLC. There were some minor peaks in the chromatograms from the fructose oxidation mixtures that eluted at earlier times, but these did not interfere with the formaldehyde adduct peak. The production of formaldehyde by glucose, galactose, and sucrose was only a small fraction (<5% for all three, data not shown) of that produced by fructose under identical conditions, as measured by the colorimetric assay.

HPLC was also used to determine whether glyoxal or methylglyoxal was the major α-dicarbonyl product in fructose degradation. Glyoxal and methylglyoxal adducts with Girard-T reagent gave peaks at 6.4 min and 8.5 min, respectively, in the chromatographic system described in Section 4. The glyoxal adduct with Girard-T reagent gave a peak that was about 15-fold larger than the peak for the methylglyoxal adduct in fructose reaction mixtures where both of these adducts were measurable. When the levels of fructose oxidation products were low (e.g., under acidic conditions) the methylglyoxal peak was too small to be integrated.

2.4. Spectrophotometric analysis of Fe(III) and Cu(II) complexes with fructose

There have been numerous reports on the complexation of iron by fructose, but we are not aware of any that studied the interaction of phosphate with the Fe(III)–fructose complex. A study of the absorption spectra of the iron and copper complexes with fructose in the wavelength range from 200 to 450 nm shows there are some subtle changes in the absorption spectrum as pH changes or as phosphate ion concentration increases from 5 mM to 100 mM at neutral pH. This complex has a broad absorption maximum in the UV spectrum

around 270 nm in neutral aqueous solutions. Under more alkaline conditions (pH 8–9), the intensity of this band decreases and there is some increase in absorbance in the 330–400 nm range, which appears as a weak

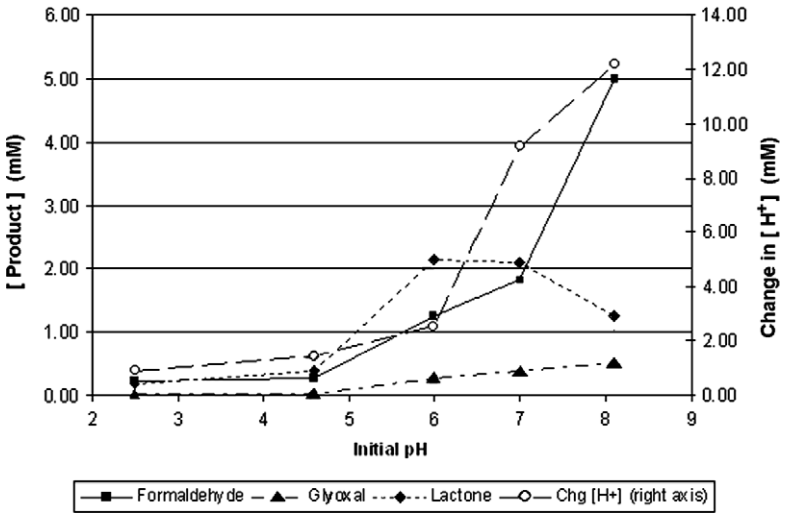

Figure 3. Dependence of the formation of four oxidation products of fructose degradation on pH between pH 2.5 and pH 8.1. Reaction mixtures contained 200 mM fructose, 20 μM $FeCl_3$, and 50 mM phosphate buffer at the designated initial pH, with 25 mM acetate added at pH 4.6 and 25 mM tris added at pH 8.1. Reaction mixtures were incubated 6 days at 40 °C prior to the analysis of oxidation products.

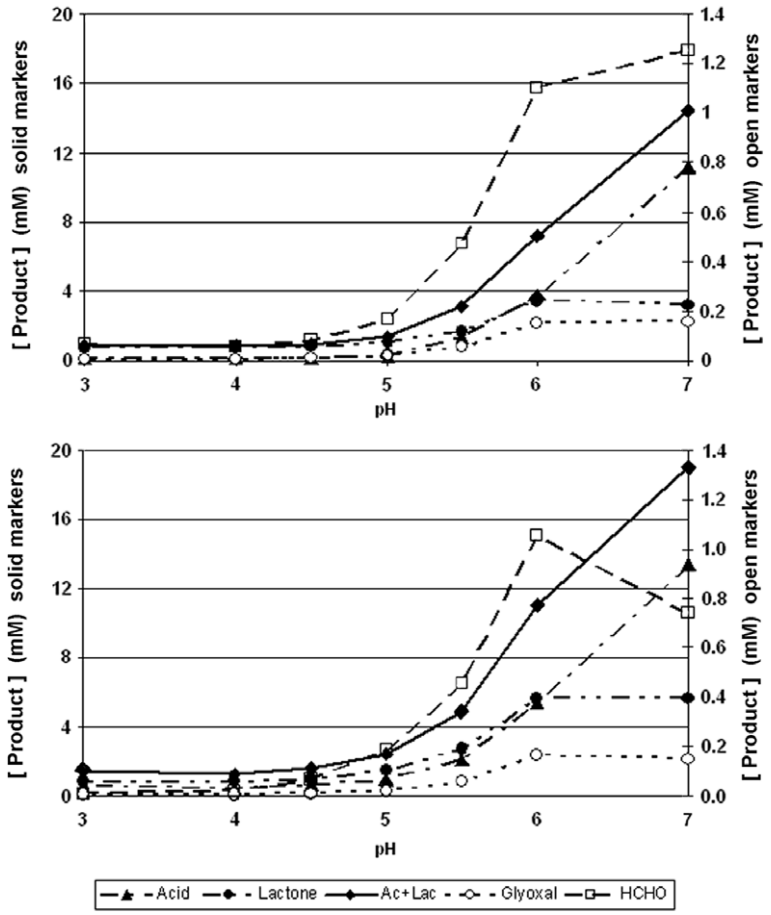

Figure 4. Comparison of Fe(III) and Cu(II) catalyzed production of oxidation products from fructose. Each reaction mixture contained 50 mM phosphate and 20 mM acetate at the designated pH. All contained 100 mM fructose, with (A) 20 μM $FeCl_3$ or (B) 20 μM $CuSO_4$ added. Reaction mixtures were incubated for 6 days at 40 °C prior to the analysis of oxidation products.

shoulder on the large UV absorption band. On the contrary, as the concentration of phosphate is increased from 5 to 100 mM at pH 7, there is a decrease in absorbance between 400 and 300 nm and an increase in the absorbance band at 270 nm, as shown in the difference spectrum (Fig. 5).

These subtle changes in the absorption spectrum of the Fe(III)–fructose complex with increasing concentration of phosphate are indicative of changes in the coordination sphere of the metal center. In view of the concentration dependent effect of phosphate on the iron catalyzed reaction, it would appear that phosphate may be coordinating the Fe(III)–fructose dimer and possibly disrupting the mu-oxo bridges proposed by Aasa et al.[11] There were also changes in the Cu(II)–fructose spectrum with changes in pH and changes in phosphate concentrations at neutral pH (data not shown). However, the copper complex precipitated from solution at neutral pH with the highest (100 mM) phosphate concentrations.

If phosphate is causing disruption of μ-oxo (or μ-hydroxo) bridging in the Fe(III)–fructose complex, an increase in the magnetic susceptibility of the complex would be expected to occur with increasing phosphate concentration. To test this hypothesis, the solution magnetic susceptibility was measured by the Evans method.[15] The solution magnetic susceptibility of the iron complex increased as the concentration of phosphate increased from 5 to 100 mM in the solutions. In the presence of 1.16 mM Fe(III) and 100 mM fructose, the shift in the upfield resonance of the methyl protons of the *iso*-propyl alcohol doublet increased as the concentration of sodium phosphate increased at pH 7.0. The calculated solution magnetic susceptibility (μ_{eff}) increased from 3.7 to 5.0 Bohr magnetons with the increase in phosphate from 5 to 100 mM (Table 3). These results would indicate that phosphate enhancement of the iron-dependent autoxidation of fructose is likely due to phosphate cleavage of the μ-oxo (or μ-hydroxo) bridging of the Fe(III)–fructose complex at neutral pH.

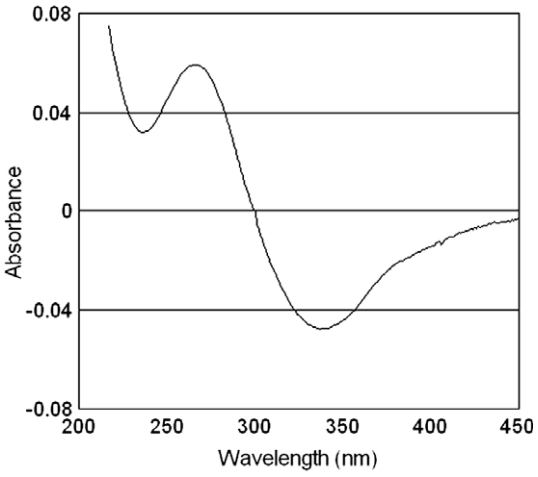

Figure 5. Difference spectrum of the Fe(III)–fructose complex in high versus low phosphate concentrations at neutral pH. The sample and reference solutions contained 100 mM fructose and 0.12 mM $FeCl_3$ at pH 7.0, with 100 mM phosphate (sample) and 5.0 mM phosphate (reference).

Table 3. Change in solution magnetic susceptibility of the Fe(III)–fructose complex with increasing phosphate concentration at neutral pH[a]

[Phosphate] (mM)	Δ[b] (Hz)	μ_{eff}[c] (Bohr magnetons)
5	5.6	3.7
20	6.4	3.9
50	8.0	4.4
100	10.6	5.0

[a] Each sample solution contained 100 mM fructose, 1.16 mM $FeCl_3$, and phosphate buffer, pH 7.0, in H_2O. Reference solutions contained only 100 mM fructose and phosphate buffer, pH 7.0, in 50% (v/v) D_2O. All solutions contained 2.5% (v/v) 2-propanol.

[b] Δ is the shift in the upfield line of the methyl protons doublet of 2-propanol in Hz.

[c] μ_{eff} is calculated as described in Section 4.

3. Discussion

The results presented here confirm earlier studies mentioned in the introduction that have shown fructose to be much more susceptible to oxidative degradation than glucose, galactose, or sucrose. The autoxidation of these sugars is dependent on the presence of redox active metal ions, as demonstrated by the strong inhibitory effect of metal chelators such as DTPA and desferrioxamine. The autoxidation of fructose in the absence of added metal ions is due to the presence of adventitious metals, particularly iron, in the purified water and buffer salts. It is common to find 10–30 ppm iron in most phosphate salts. Consequently, 100 mM phosphate solutions would contain >1 μM iron and perhaps as much as 4 μM. It was found that the addition of as little as 10 μM DTPA or desferrioxamine to phosphate buffered solutions completely inhibited fructose oxidation in the absence of added metals.

This study has shown that fructose autoxidation generates both superoxide and hydroxyl radicals. In addition, there was a good correlation between hydroxyl radical generation (measured by the production of fluorescence products from benzoate ion) and production of oxidized organic species, including α-dicarbonyls, formaldehyde, acids, and lactones. Glyoxal was identified as a major α-dicarbonyl product by HPLC analysis of the Girard-T reagent derivatives in the fructose reaction mixtures, in agreement with Wells-Knecht et al.[16] who showed glyoxal to be the only low molecular weight α-dicarbonyl to be formed from glucose oxidation. Methyl glyoxal was found to be a minor product in fructose oxidation in this study. Other dicarbonyls were not identified.

This is the first study we are aware of that has identified formaldehyde as a major product of fructose degradation, with more than 1 mM formaldehyde measured in reaction mixtures containing high (0.1 M) fructose over a period of one week at 40 °C. Khan et al.[17] alluded to identification of the 2,4-dinitrophenylhydrazone derivative of formaldehyde in the vanadium(V) catalyzed oxidation of fructose, but no data were presented. The fact that acidic conditions strongly suppress fructose autoxidation bodes well for the stability of fructose in many foods and beverages, most of which tend to be acidic. However, there is still some oxidation of fructose taking place in acidic solutions and these oxidation products may be of some concern, for example, 40 μM formaldehyde (>1 ppm) was produced in one day at 40 °C in reaction mixtures containing 200 mM fructose and 50 mM phosphate at pH 2.5.

In the case of the Cu(II)–fructose complex, Cerchiaro et al.[14] have indicated Cu(II) binding to both pyranose and furanose forms of fructose in the solid state, with preference for the furanose structure, based on Raman spectroscopy. Their elemental analysis of the solid complex was consistent with a formula of $Na_2[Cu_3(fructose)_4]\cdot 8H_2O$ with Cu(II) coordinated to the C-1 and C-2 OH groups. However, Aasa et al.[11] concluded from electron paramagnetic resonance and NMR data that the Cu(II)–fructose complex was best represented as a monomeric species with two fructose ligands per Cu(II) ion in solution. If the latter structure is correct for the complex in solution, it may be that high concentrations of phosphate promote a disruption of the coordination sphere of Cu(II) to facilitate fructose oxidation. This is supported by changes in the Cu(II)–fructose spectrum when phosphate concentration increases. Desferrioxamine (10 μM) was added to solutions when assessing Cu(II) catalyzed oxidations in the present study to suppress the effects of traces of iron that would be present in the phosphate salts. This concentration of desferrioxamine was found to completely suppress fructose oxidation at 100 mM phosphate in the absence of added metal ions.

The catalytic effect of phosphate on sugar autoxidation has been known for nearly a century.[6,7] It was shown here that iron chelating agents, particularly DTPA and desferrioxamine, which are known to strongly suppress iron catalyzed oxidations, will almost completely inhibit fructose autoxidation, even in the presence of high phosphate concentrations. The nature of the Fe(III)–fructose complex appears to be controversial in terms of the structure of coordinated fructose, that is, whether fructose is in the pyranose, furanose, or straight chain ketone form when coordinated to iron. There is evidence from ^{13}C NMR spectroscopy that Fe(III) coordinates the β-pyranose form of fructose preferentially in aqueous solutions at room temperature.[13] Rao et al.[12] proposed a complex with a single μ-oxo bridge and two fructose ligands per Fe(III) center, based on elemental analysis of their solid complex. The Rao group later proposed a μ-hydroxo dimer based on their solid state magnetic susceptibility measurements and antiferromagnetic coupling constants.[18] Our observed solution magnetic susceptibility of 3.7 Bohr magnetons at the lowest (5 mM) phosphate concentration is in good agreement with that measured by Aasa et al.[11] in the absence of phosphate at neutral pH. It has been suggested that magnetic susceptibilities in this range are indicative of iron(III) complexes with μ-hydroxo rather than μ-oxo bridging.[18]

From the results of the present study, it is postulated that phosphate disrupts the μ-oxo (or μ-hydroxo) bridging of the Fe(III)–fructose dimer, as shown in Scheme 1, making the Fe(III) center more reactive or susceptible to reduction by fructose (either coordinated fructose or free fructose in solution). This is supported by the observed changes in the UV spectrum of the

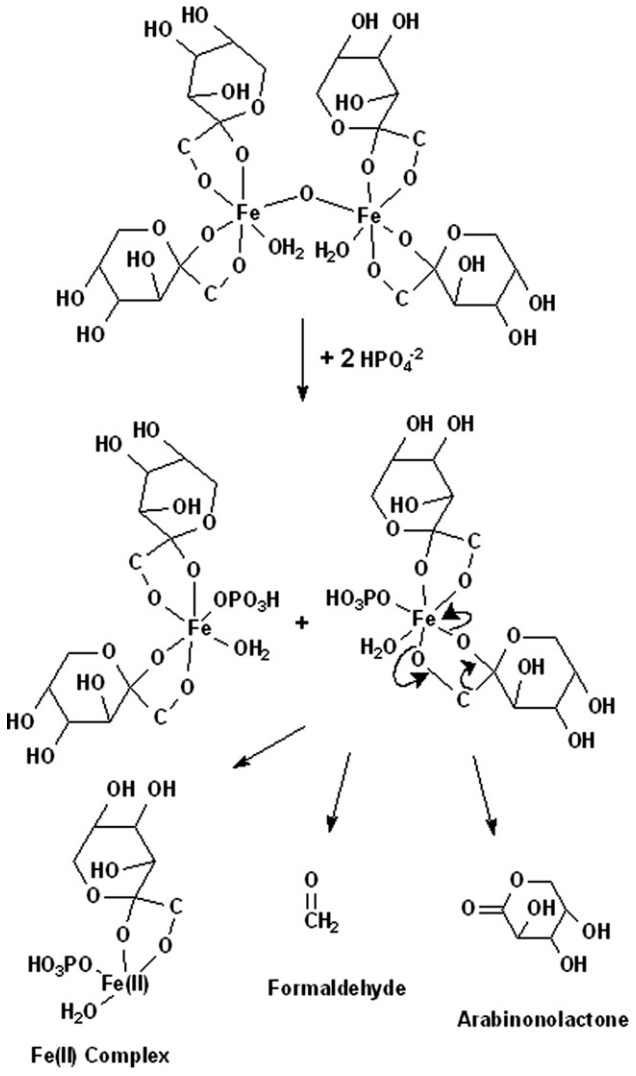

Scheme 1.

Fe(III)–fructose complex, as well as the increase in solution magnetic susceptibility when phosphate concentration is increased. In this scheme, the rearrangement of electrons in the Fe(III)–fructose–phosphate complex results in the formation of formaldehyde, arabinonolactone, and a Fe(II) complex that can react with oxygen to produce reactive oxygen species (ROS) such as superoxide and hydroxyl radicals. Further studies are needed to better characterize additional products of fructose oxidation, particularly shorter chain carbohydrate fragments (e.g., arabinonolactone) to produce a more complete mechanism for fructose degradation.

4. Experimental

4.1. Lipid peroxidation

Liposomes were prepared by dissolving 0.15 g soy lecithin in 1 mL chloroform, evaporating the chloroform under a stream of purified N_2 to form a thin film of lipid on the walls of a 125 mL Erlenmeyer flask and 60 mL of deaerated double strength phosphate buffered saline (PBS), pH 7.4 was added and the mixture sonicated in a water bath sonicator for 15 min. Liposome suspension (2.5 mL) was transferred to screw cap test tubes and fructose or glucose solution and $FeCl_3$ or $CuSO_4$ solutions were added to give the desired concentrations in a final volume of 3.0 mL. Each sample was prepared in triplicate. The suspensions were capped and mixed well before incubating in an oven at 40 °C. At the designated times, 0.4 mL aliquots were transferred to microfuge tubes and 0.8 mL of solution containing 0.375% (w/v) thiobarbituric acid (TBA) and 15% (w/v) trichloroacetic acid in 0.25 M HCl was added. The mixture was heated in a boiling water bath for 15 min, cooled and centrifuged at 2000 rpm for 5 min. The absorption of the supernatant liquid was measured at 535 nm in a Jasco V-530 spectrophotometer versus a blank prepared by adding 0.4 mL PBS to 0.8 mL TBA reagent and heating as for samples.

4.2. Free radical production

4.2.1. Hydroxyl radical production. Sodium benzoate stock solution (100 mM) was prepared by dissolving 1.22 g benzoic acid (0.01 mol) and 0.40 g sodium hydroxide (0.01 mol) in distilled water, brought to 100 mL and stored at 4 °C until needed. Fructose, glucose, and other carbohydrate stock solutions were prepared by dissolving the respective sugar in distilled water just prior to mixing of test reaction mixtures. Reaction mixtures contained a final concentration of 5.0 mM sodium benzoate with varying amounts of sugar, varying concentrations of phosphate buffers at their respective pH values, and varying concentrations of disodium ethylenediaminetetraacetic acid (EDTA), diethylenetriaminepentaacetic acid (DTPA), desferal mesylate (Ciba-Geigy), $FeCl_3$, or $CuSO_4$. Reaction mixture fluorescence was measured on a Shimadzu RF5301PC spectrofluorometer with excitation at 298 nm and emission at 403 nm, which corresponds to the wavelengths for maximum excitation and emission for sodium salicylate. The *meta*- and *para*-hydroxybenzoate isomers have similar excitation and emission spectra.[19] Salicylate standards ranging from 0.50 to 250 μM were prepared by dilutions in phosphate buffered saline, pH 7.4, of a 10.0 mM salicylic acid stock solution. The fluorescence intensity of salicylate standards in this concentration range showed good linearity ($r^2 > 0.99$).

4.2.2. Superoxide production. Nitrobluetetrazolium (NBT, Sigma) stock solution (10 mM in water) was added to 20 mM sugar solutions containing 50 mM phosphate buffer at the indicated pH. The final concentration of NBT was 0.5 mM in the reaction mixtures, which contained 20 μM $FeCl_3$ as catalyst. Reduction of NBT by superoxide was monitored by measuring absorbance at 560 nm on a JASCO V-530 spectrophotometer. Superoxide dismutase was isolated from human red blood cells and enzyme activity assayed by the inhibition of 6-hydroxydopamine autoxidation.[20] After 24 h the qualitative differences in superoxide production were apparent by comparing the blue color of the monoformazan to the yellow color of the nitrobluetetrazolium dication, as well as by measuring absorbance at 560 nm. Quantification of yield from superoxide scavenging is improved by dilution in dimethyl sulfoxide, because of the low solubility of the reduced monoformazan product in water.

4.3. Measurement of oxidation products

4.3.1. Formaldehyde production. Formaldehyde was measured by the Hantzsch reaction using Nash reagent according to the method of Anton and Barrett.[21] Formaldehyde standards were prepared by dilution of 40% formalin solution in phosphate buffered saline and showed good linearity over the concentration range of 0–0.70 mM with molar absorptivity of 8000 M^{-1} cm^{-1}, in agreement with Nash.[22] The product being assayed by this procedure was confirmed to be formaldehyde by liquid chromatography of the acetylacetone adduct of formaldehyde on a Waters Xterra RP18, 5 μm column, 4.6 × 250 mm using a mobile phase consisting of 80% of 20 mM ammonium acetate, pH 6.2, and 20% methanol at a flow rate of 1.0 mL per min. Absorbance of eluent was monitored at 410 nm.

4.3.2. α-Dicarbonyl production. A 100 μL aliquot of reaction mixture was mixed with 50 μL of 0.50 M

Girard-T reagent (aqueous) and 850 μL of 0.5 M sodium formate buffer, pH 2.9, according to the method of Mitchel and Birnboim.[23] The mixture was incubated at room temperature for 15 min and the absorbance measured at 295 nm versus a reagent blank containing 100 μL phosphate buffer in the place of reaction mixture. Dicarbonyl adducts of Girard-T reagent were analyzed by liquid chromatography using a modification of the procedure of Wells-Knecht et al.[16] The liquid chromatography system consisted of a Metachem C8-ether, 3 μm column, 4.6 × 250 mm, using a mobile phase consisting of 0.10 M propionic acid adjusted to pH 5.2 with sodium hydroxide at a flow rate of 1.0 mL per min. Absorbance of eluent was monitored at 295 nm.

4.3.3. Lactone production. Hydroxylamine hydrochloride will react with acyl anhydrides, esters, and lactones, and to a lesser extent with amides, forming hydroxamic acids that form a purplish complex with iron under acidic conditions.[24,25] Free acids do not give this reaction. Since anhydrides and amides would not be formed in these reaction mixtures, the main products measured in this assay would be lactones, and perhaps esters. Hydroxylamine hydrochloride (28%, 4 M) is mixed with an equal volume of 14% (3.5 M) NaOH solution to nearly neutralize the hydrochloride. An aliquot (200 μL) of fructose reaction mixture is mixed with 200 μL of the neutralized hydroxylamine solution and 200 μL of 0.10 M sodium acetate buffer, pH 5.6, and allowed to stand at room temperature for 10 min, then 200 μL of 3 M HCl and 200 μL of 5% $FeCl_3$ (monohydrate) in 0.1 M HCl were added. The absorbance was measured at 510 nm versus a blank containing phosphate buffered saline in the place of the fructose reaction mixture. The blank assay mixture was yellow in color and gave absorbance of less than 0.02.

4.4. Spectrophotometric analysis of fructose complexes

The absorption spectrum of the Fe(III) and Cu(II) complexes was recorded in weakly acidic, neutral, and weakly alkaline solutions and at high or low concentrations of phosphate. All solutions for spectral analysis contained 100 mM fructose with 0.10 mM $FeCl_3$ or 0.10 mM $CuSO_4$ and 5.0 or 100 mM phosphate buffer at the indicated pH. The final pH was adjusted with dilute NaOH solutions. Absorption spectra were recorded on a Bio-Crom 8500 II dual-beam spectrophotometer with water as reference. Difference spectra were recorded where indicated.

4.5. Solution magnetic susceptibility

The magnetic susceptibility of the Fe(III)–fructose complex was measured by the Evans method[15] using coaxial NMR tubes (inner tube: 2.34 mm ID, 3.30 mm OD; outer tube: 4.20 mm ID, 4.97 mm OD). Solutions containing 100 mM fructose and 5.0, 20, 50, or 100 mM sodium phosphate buffer, pH 7.0, 0.35 M 2-propanol and 50% D_2O were placed in the inner coaxial NMR tube. Identical solutions with 1.16 mM $FeCl_3$ added were placed in the outer coaxial NMR tube. NMR spectra of the solutions with and without iron were recorded simultaneously on a Varian 400 MHz NMR spectrometer. Normally, *tert*-butyl alcohol is used as the inert organic compound for solution magnetic susceptibility measurements, but this alcohol caused precipitation of the Fe(III)–fructose complex at high phosphate concentrations, whereas *iso*-propyl alcohol solutions remained clear at room temperature. The solution magnetic susceptibility was calculated from the shift of the downfield line for the *iso*-propyl group doublet.[26]

Acknowledgments

G.D.L. extends special thanks to Professor Hasan Seçen, Department of Chemistry, Arts and Sciences Faculty, Ataturk University, for the invitation to spend a sabbatical year at that institution and for many helpful discussions regarding this research. Thanks to Ali Yildirim, head of Chemistry Education in the Kazim Karabakir Education Faculty at Ataturk University for the laboratory facilities to carry out this research, and to Dr. Cavit Kazar, Department of Chemistry, Arts and Sciences Faculty, Ataturk University and Dr. Samuel Watson, Department of Chemistry and Biochemistry, Long Island University for assistance with the NMR analyses. GDL also thanks Long Island University for granting a sabbatical year to pursue this research.

References

1. Bray, G. A.; Nielsen, S. J.; Popkin, B. M. *Am. J. Clin. Nutr.* **2004**, *79*, 537–543.
2. Elliott, S. S.; Keim, N. L.; Stern, J. S.; Teff, K.; Havel, P. J. *Am. J. Clin. Nutr.* **2002**, *76*, 911–922.
3. Hollenbeck, C. B. *Am. J. Clin. Nutr.* **1993**, *58*, 800S–809S.
4. Faure, P.; Rossini, E.; Lafond, J. L.; Richard, M. J.; Favier, A.; Halimi, S. *J. Nutr.* **1997**, *127*, 103–107.
5. Sakai, M.; Oimomi, M.; Kasuga, M. *Kobe J. Med. Sci.* **2002**, *58*, 125–136.
6. Spoehr, H. A. *J. Am. Chem. Soc.* **1924**, *46*, 1494–1502.
7. Witzemann, E. J. *J. Biol. Chem.* **1920**, *45*, 1–22.
8. Clinton, M., Jr.; Hubbard, R. S. *J. Biol. Chem.* **1937**, *119*, 467–472.
9. Bunn, H. F.; Higgins, P. J. *Science* **1981**, *213*, 222–224.
10. Charley, P. J.; Sarkar, B.; Stitt, C. F.; Saltman, P. *Biochim. Biophys. Acta* **1963**, *69*, 313–321.
11. Aasa, R.; Malmstrom, B.; Saltman, P.; Vanngard, T. *Biochim. Biophys. Acta* **1964**, *80*, 430–437.
12. Rao, C. P.; Geetha, K.; Raghavan, S. S. *BioMetals* **1994**, *7*, 25–29.
13. Tonkovic, M. *Carbohydr. Res.* **1994**, *254*, 277–280.

14. Cerchiaro, G.; Sant'Ana, A. C.; Temperini, M. L. A.; da Costa Ferreira, A. M. *Carbohydr. Res.* **2005**, *340*, 2352–2359.
15. Evans, D. F. *J. Chem. Soc.* **1959**, 2003–2005.
16. Wells-Knecht, K. J.; Zyzak, D. V.; Litchfield, J. E.; Thorpe, S. R.; Baynes, J. W. *Biochemistry* **1995**, *34*, 3702–3709.
17. Khan, Z.; Babu, P. S.; Kabir-ud-Din *Carbohydr. Res.* **2004**, *339*, 133–140.
18. Geetha, K.; Raghavan, M. S. S.; Kulshreshtha, S. K.; Sasikala, R.; Rao, C. P. *Carbohydr. Res.* **1995**, *271*, 163–175.
19. Gutteridge, J. M. C. *Biochem. J.* **1987**, *243*, 709–714.
20. Mavi, A.; Kufrevioglu, O. I.; Yildirim, A. *J. Enz. Inhib. Med. Chem.* **2006**, *21*, 235–239.
21. Anton, G. E.; Barrett, D. M. *J. Agric. Food Chem.* **2004**, *52*, 3749–3753.
22. Nash, T. *Biochem. J.* **1953**, *55*, 416–421.
23. Mitchel, R. E. J.; Birnboim, H. C. *Anal. Biochem.* **1977**, *81*, 47–56.
24. Lipmann, F.; Tuttle, L. C. *J. Biol. Chem.* **1945**, *159*, 21–28.
25. Hestrin, S. *J. Biol. Chem.* **1949**, *180*, 249–261.
26. Helman, R.; Lawrence, G. D. *Bioelectrochem. Bioenerget.* **1989**, *22*, 187–196.